

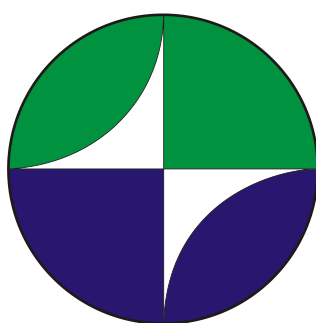
**RUSSIAN ACADEMY OF SCIENCES**  
**NATIONAL GEOPHYSICAL COMMITTEE**  
**РОССИЙСКАЯ АКАДЕМИЯ НАУК**  
**НАЦИОНАЛЬНЫЙ ГЕОФИЗИЧЕСКИЙ КОМИТЕТ**



**NATIONAL REPORT**  
for the  
International Association for  
the Physical Sciences of the Oceans  
of the  
International Union of Geodesy and Geophysics  
2007–2010

**НАЦИОНАЛЬНЫЙ ОТЧЕТ**  
Международной ассоциации физических наук об  
океане  
Международного  
геодезического и геофизического союза  
2007–2010

**Москва 2011 Moscow**



**Presented to the XXV General Assembly  
of the  
International Union of Geodesy and Geophysics**

**К XXV Генеральной ассамблее  
Международного геодезического и геофизического  
союза**

**RUSSIAN ACADEMY OF SCIENCES**

National Geophysical Committee

**NATIONAL REPORT**

for the

International Association for  
the Physical Sciences of the Oceans

of the

International Union of Geodesy and Geophysics

2007–2010

Presented to the XXV General Assembly

of the

IUGG

2011

Moscow

This report submitted to the International Association for the Physical Sciences of the Oceans (IAPSO) of the International Union of Geodesy and Geophysics (IUGG) contains results obtained by Russian scientists in 2007–2010.

Editorial Board

E.G. Morozov (*Chief Editor*).

© 2011 National Geophysical Committee of Russia

## Contents

Variability and renewal of Labrador Sea Water in the Irminger Basin in 1991–2004.....	6
Monitoring of temperature and salinity along 60°N.....	7
Transport by the Deep Western Boundary Current.....	8
Flows in the abyssal channels of the Atlantic Ocean.....	9
Currents in the Drake Passage and Scotia Sea.....	10
Circulation in the Southwestern Part of the Kara Sea in September 2007.....	11
Strong internal tides in the Kara Gates Strait.....	12
Zonality in the Kara Sea shelf.....	13
Research in the Black Sea.....	14
Wave interactions.....	15
Internal waves under ice.....	15
Satellite oceanography.....	16
Radar observations of the surface.....	16
Mathematical modeling.....	17
Caspian Sea.....	18
Global circulation model.....	20
Laboratory modeling.....	21
Laboratory experiments.....	21

## Variability and renewal of Labrador Sea Water in the Irminger Basin in 1991–2004

Labrador Sea Water (LSW) property variations are analyzed using the data from six hydrographic sections occupied in 1991–2004 in the southern Irminger Basin between Cape Farewell and the Reykjanes Ridge. From 1991 to 1996, the LSW layer became steadily colder and fresher. The decrease in salinity of the LSW detected in 1994 was caused by the local convection, reaching into the weakly stratified layer of LSW advected from the Labrador Sea. Another indication of local deep convection is in the lateral distribution of dissolved oxygen concentrations in the LSW layer (1000–2000 m) obtained in 1997 from the section across the Labrador Sea and four sections running 100, 135 and 180 (true azimuth) from Cape Farewell. A separate lateral maximum of oxygen content in the LSW layer is revealed in the southern Irminger Sea: the concentrations increased from the Labrador Sea eastern edge toward the Irminger Sea rather than the reverse, as would be expected if there was no local modification of LSW by deep convection. Since 1996, the two-modal structure of LSW has been observed in the Irminger Basin. The upper mode of LSW detected in 1996 was formed in situ; during the winter of 1996/1997, the upper mode was locally renewed. From 1997 to 2004, the temperature and salinity signatures of the deeper mode considerably eroded due to the lack of the renewal of the deeper LSW reservoir in the Labrador Sea, while the annually renewed upper mode, on the contrary, became more pronounced.

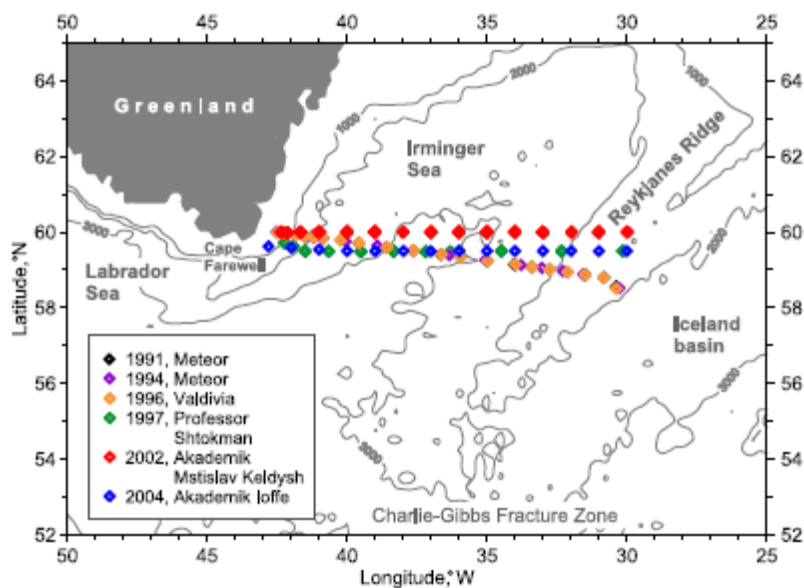


**Figure.** Locations of the hydrographic sections in the Irminger Sea.

## Monitoring of temperature and salinity along 60°N

It was found on the basis of the annual (1997-2010) monitoring of temperature and salinity over the hydrographic section along 60° N and application of the historical data that long-term variations in the temperature and salinity of the deep limb of the global inter-ocean circulation are caused by the natural fluctuations of the atmospheric pressure over the North Atlantic (North Atlantic Oscillation, NAO). Displacement of subsurface currents and variations in the intensity of convection caused by the variations in the pressure difference between the Azores Islands and Iceland lead to the correlated fluctuations of temperature and salinity at depths from 500-1000 m to the bottom.

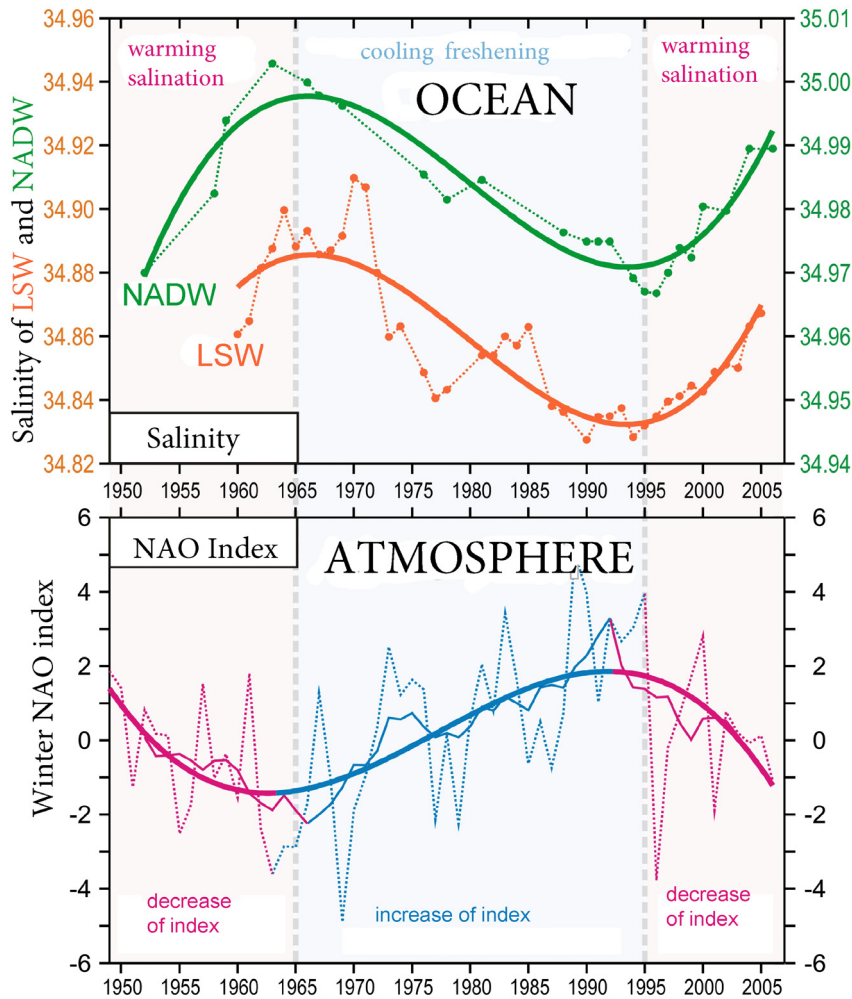


**Figure.** Variations in salinity (psu) of Labrador Sea water (LSW) and North Atlantic Deep Water (NADW) in the regions of their formation (above). Variations in the North Atlantic Oscillation index (NAO) (below). The low-frequency components of variations are shown with the cubic polynomials. The low frequency component of the NAO is shown using the 7-year running averaging (thin solid line) and cubic polynomial (thick line).

## Transport by the Deep Western Boundary Current

Analysis of the time series of baroclinic transport by the Deep Western Boundary Current (1955-2007) allowed us to find a close correlation (negative) between the transport by the current and thickness of the convective layer in the Labrador Sea. It was found that the variations in the transport by the Deep Western Boundary Current are retarded by 1-3 years with respect to the variations in the intensity of deep convection in the Labrador Sea, which agrees with the results of numerical modeling of circulation in the North Atlantic, according to which the Subpolar gyre responds to the variations in the convection intensity with a time lag of  $\sim 3$  years.

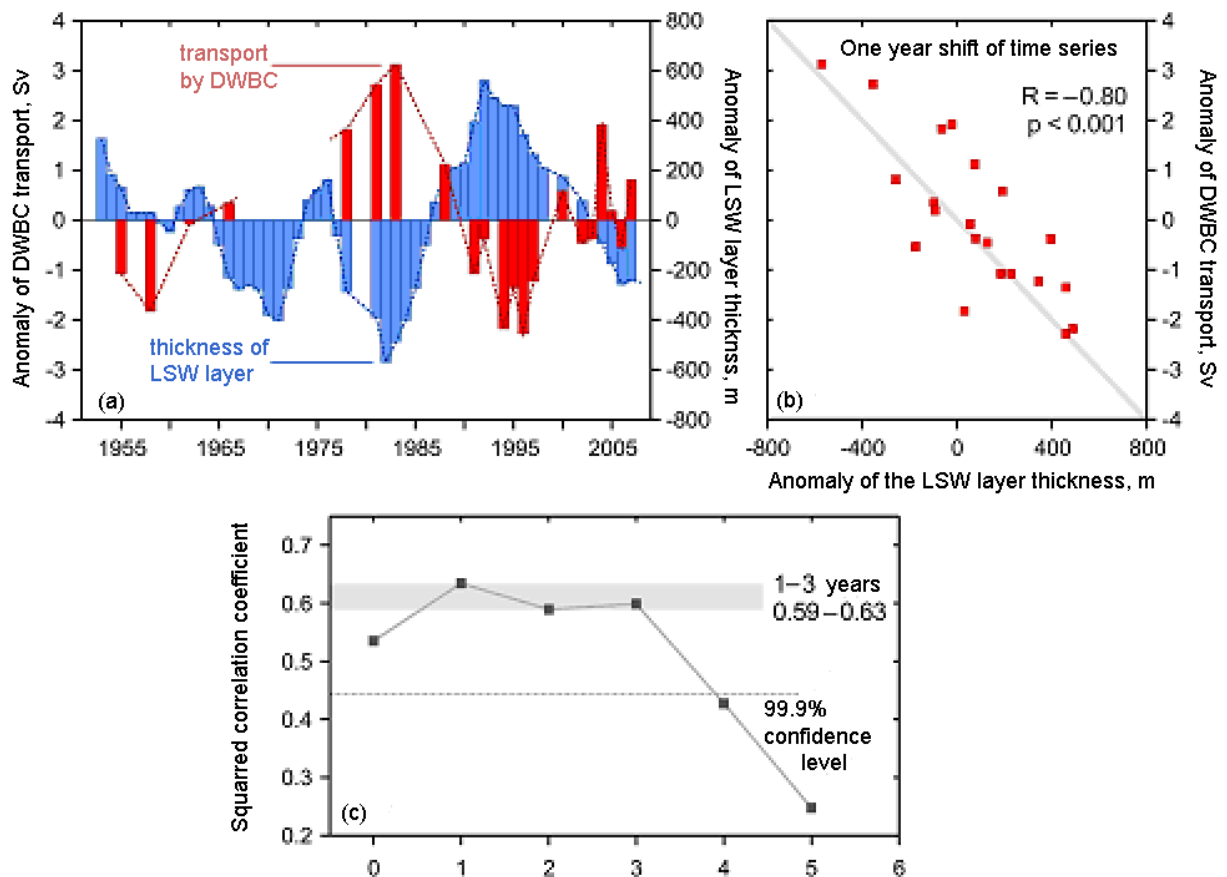


**Figure.** Time series (1955-2007) of the anomalies of geostrophic DWBC transport (Sv) in the southern part of the Irminger Sea extended from the paper by Bacon [1998] and anomalies of the LSW thickness (m) in the central part of the Labrador Sea extended from the paper by Curry [1998]. Correlation between anomalies of the DWBC transport and anomalies of the LSW layer thickness if the shift between the time series is one year. The thickness of the LSW is ahead. Correlation between the DWBC transport and LSW thickness as function of the shift between the time series (years). The thickness of the LSW advances.

## Flows in the abyssal channels of the Atlantic Ocean

A strong flow of Antarctic Bottom Water from the Argentine Basin to the Brazil Basin through the Vema Channel (32°-27° S) is studied on the basis of CTD sections combined with LADCP profiling carried out annually and long-term moored measurements. The flow in the Vema Channel is mixed in the vertical direction but horizontally stratified. The mean speed of the flow is 30 cm/s and water transport is approximately 3.5 Sv. Owing to the bottom Ekman friction the dense core of the flow is usually displaced to the eastern wall of the channel. A temperature increase was found in the deep Vema Channel, which has been observed for 30 years already.

The further flow of bottom water in the Brazil Basin splits in the northern part of the basin. Part of water flows to the East Atlantic basins through the Romanche and Chain fracture zones. The other part is a northwestern flow to the North American Basin. Part of the northwesterly flow propagates through the Vema Fracture Zone (11° N) into the Northeastern Atlantic basins.

Flows in the Romanche, Chain, and Vema fracture zones were studied recently by CTD and LADCP profiling. An underwater cataract was found in the Chain fracture Zone. Recent measurements in the Kane Gap show that the flow of bottom water there is characterized by alternative transport in time. The Northeastern Atlantic basins are filled with the bottom water flowing through the Vema Fracture Zone. The flows of bottom waters through the Romanche and Chain fracture zones do not spread to the Northeast Atlantic due to strong mixing in the equatorial zone and enhanced transformation of bottom water properties.

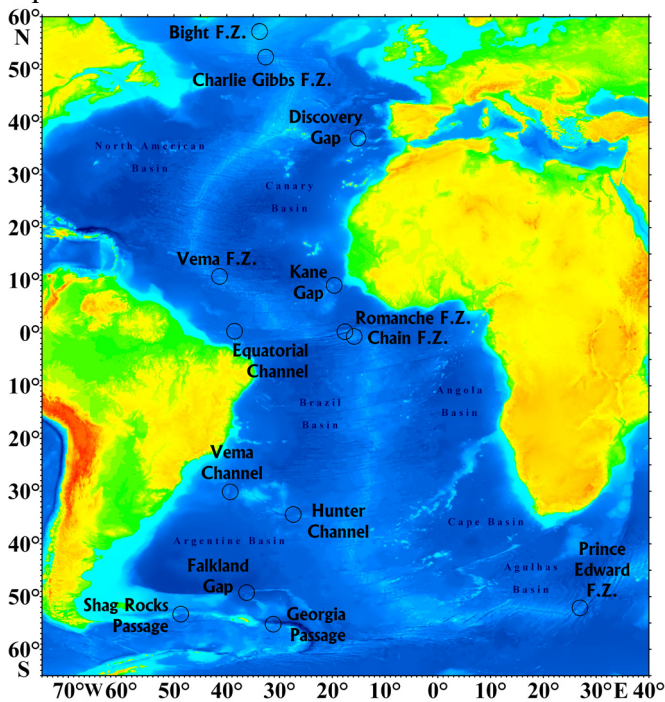


**Figure.** Chart of the Atlantic Ocean showing the location of the major abyssal channels mostly associated with fracture zones

## Currents in the Drake Passage and Scotia Sea

New results on the intensity and circulation structure in the Drake Passage and Scotia Sea were obtained on the basis of systematic field measurements carried out by the Shirshov Institute of Oceanology since 2003 and foreign data. High velocities of bottom currents (up to 45 cm/s) were found. The influence of the bottom topography on the currents was revealed and new pathways of deep and bottom water propagation were found.

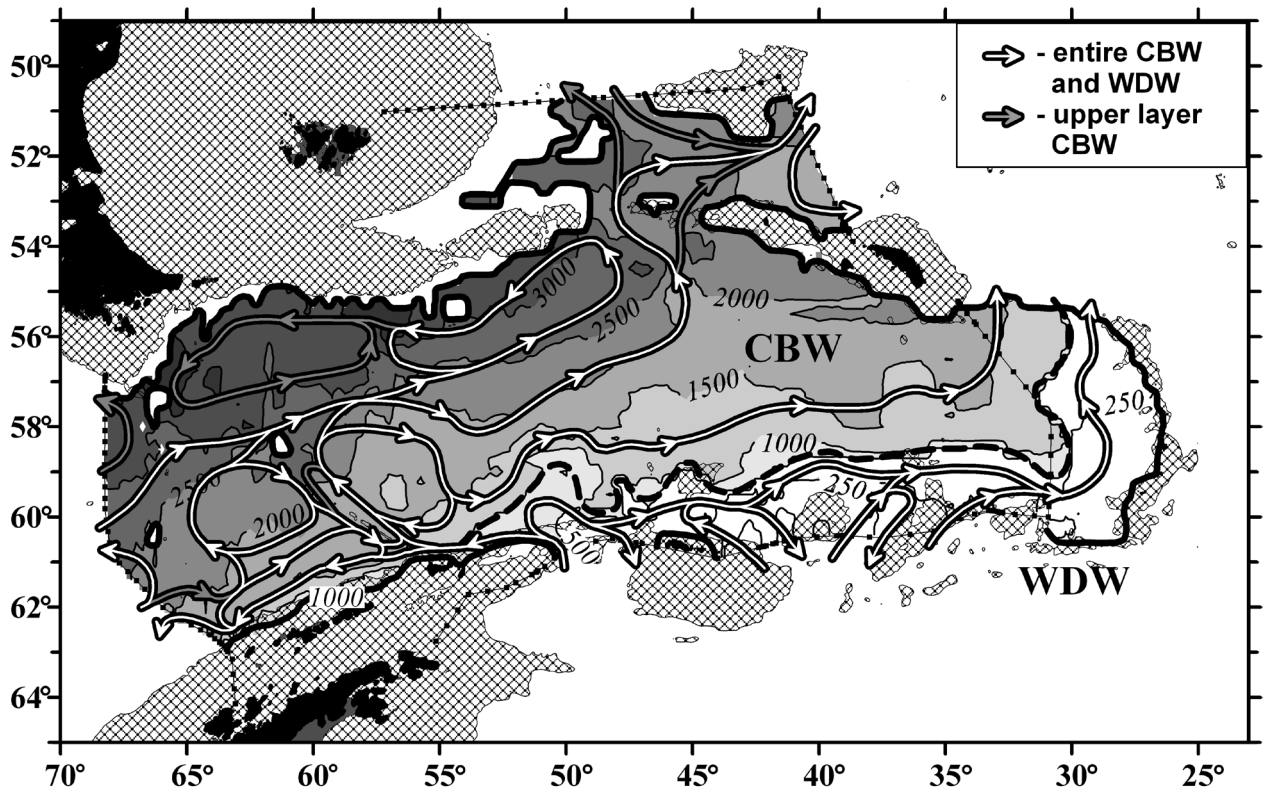


**Figure.** Topography of the upper boundary surface of Circumpolar Bottom Water and Warm Deep Water (m) in the Drake Passage and Scotia Sea. Regions with depths shallower than 2000 m are dashed. Arrows show the scheme of Circumpolar Bottom Water and Warm Deep Water spreading in the region. Thick dashed line divides the spreading regions of CBW and WDW.

## Circulation in the Southwestern Part of the Kara Sea in September 2007

During cruise 54 of the R/V *Akademik Mstislav Keldysh* to the southwestern Kara Sea (September 6 to October 7, 2007), a large amount of hydrophysical data with unique spatial resolution was obtained on the basis of measurements using different instruments. The analysis of the data gave us the possibility to study the dynamics and hydrological structure of the southwestern Kara Sea basin. The main elements of the general circulation are the following: the Yamal Current, the Eastern Novaya Zemlya Current, and the St. Anna Trough Current. All these currents are topographically controlled; they flow over the bottom slopes along the isobaths. The Yamal Current begins at the Kara Gates Strait and turns to the east as part of the cyclonic circulation. Then, it turns to the north and propagates along the Yamal coast over the 100-m isobath. The Eastern Novaya Zemlya Current (its core is located over the eastern slope of the Novaya Zemlya Trough) flows to the northeast. Near the northern edge of Novaya Zemlya, it encounters the St. Anna Trough Current, separates from the coast, and flows practically to the east merging with the continuation of the Yamal Current. A strong frontal zone is formed in the region where the two currents merge above the threshold that separates the St. Anna Trough from the Novaya Zemlya Trough and divides the warm and saline Arctic waters from the cooler and fresher waters of the southwestern part of the Kara Sea. This threshold, whose depth does not exceed 100–150 m, is a barrier that prevents the spreading of the Barents Sea and Arctic waters to the southwestern part of the Kara Sea basin through the St. Anna Trough.

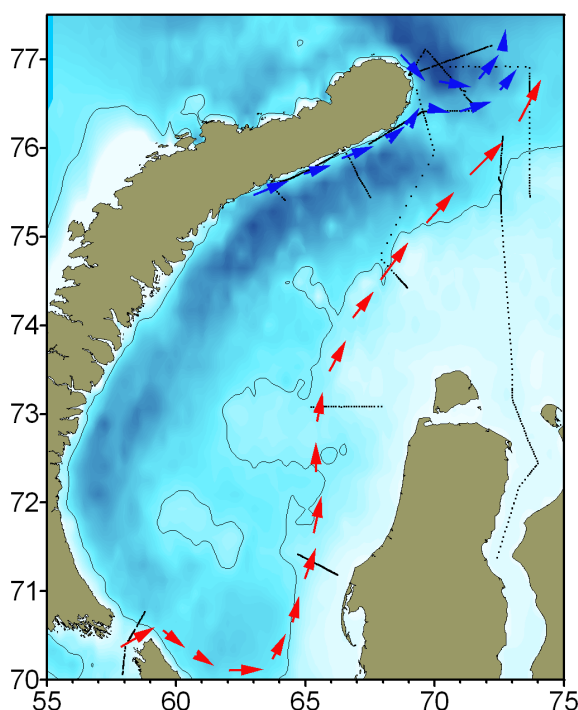


**Figure.** The average current vectors (segments of a straight line) in the layer between 15 and 45 m based on the data of the measurements with a towed ADCP along the sections in different regions of the southwestern part of the Kara Sea and a scheme of the circulation in the upper 10-m layer in the southwestern part of the Kara Sea based on the observations in September 2007. The arrows show the main currents. The solid line denotes the 100-m isobath.

## Strong internal tides in the Kara Gates Strait

We analyze towed CTD measurements, numerical model calculations, and radar images in the Strait of Kara Gates. The measurements were made during an expedition in September 2007. Strong internal tides propagating from the Kara Strait to the Barents Sea were recorded. The internal waves are intensified by the opposite current from the Barents Sea. An internal bore followed by a packet of short-period internal waves was found southwest of the strait. Radar images show that short-period internal waves are generated after the internal bore. A hydraulic jump was found on the eastern side of the strait. Numerical modeling agrees with the experimental results.

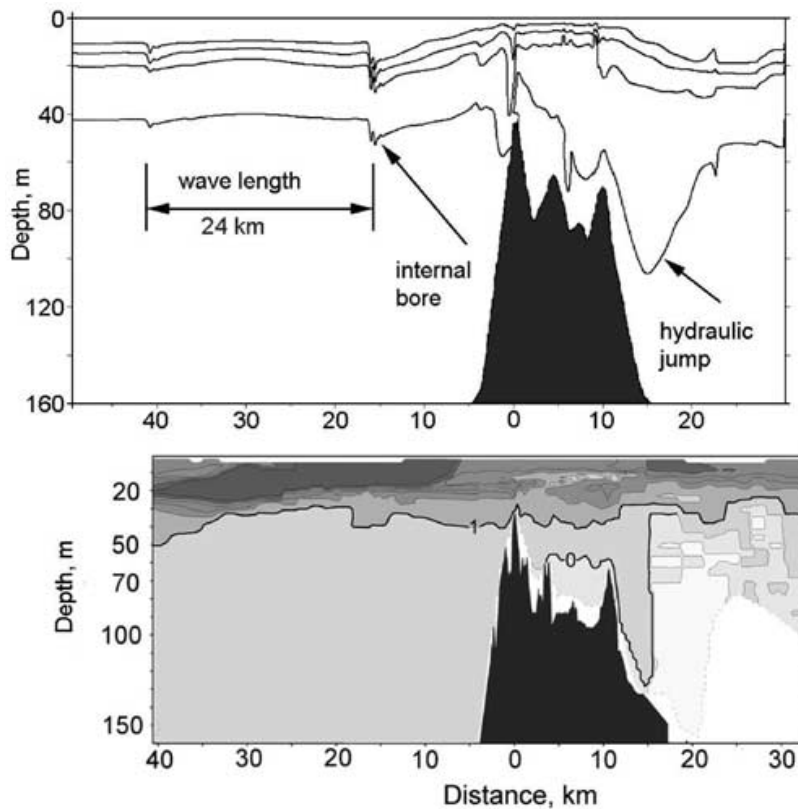


**Figure:** Field of isopycnals 23.5, 24.5, 25.5, and 26.5 perturbed by the flow in the strait and internal waves based on the numerical calculations. Black color shows the bottom topography as specified in the model (top). Distribution of temperature over the towed section. Isotherms are shown with an interval of 1°C. Thicker lines show isotherms of 1 and 0°C to emphasize the observed effect. Black color shows the bottom profile (bottom).

## Zonality in the Kara Sea shelf

The studies in the shelf and continental slope of the Kara Sea demonstrated that the inner shelf front associated with the estuary zone of the Ob River determines the cross-shelf zonality. It is a barrier zone that restricts the transport in the system shelf - continental slope - deep basin. It also restricts the influence of the shelf ecosystem on the ecosystems of the deep Arctic basin. A sharp change in the species structure of the phyto- and mesoplankton communities is associated with the inner shelf front. A multi-fold (up to 10 times reaching  $12 \text{ g/m}^3$ ) increase of the total biomass of mesoplankton forming a powerful frontal biological filter is also related to the inner shelf. The frontal change in the environment and structure of pelagic ecosystems is associated with a sharp increase in salinity in the surface layer (from 3 to 8 psu) and in the bottom layer (from 15 to 20 psu).

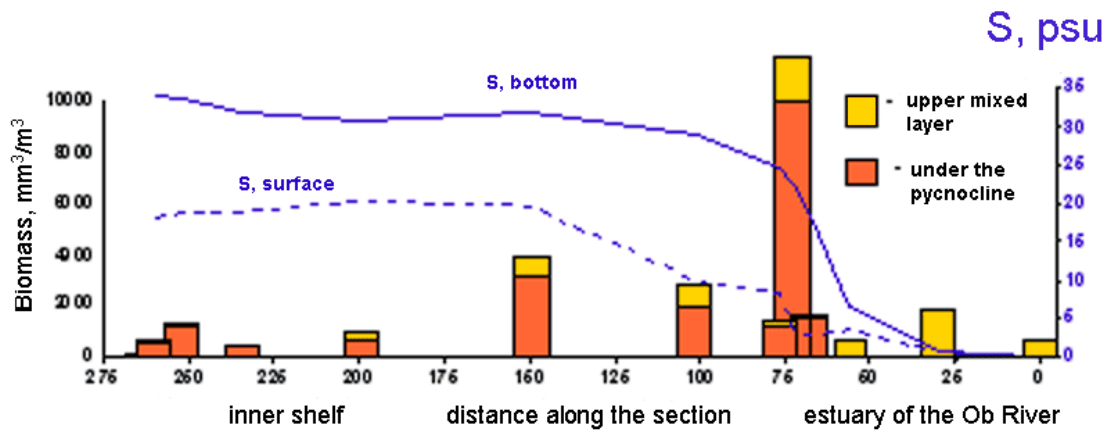


**Figure.** Manifestation of the inner frontal zone in the mesoplankton biomass and salinity distribution over the section across the shelf to the continental slope.

## Research in the Black Sea

Investigations of the spatiotemporal variability of hydrophysical parameters in the sea over the shelf and upper part of the continental slope of the Black Sea revealed significant mesoscale variability of currents that evidences the fact of intense water exchange in the shelf region that ventilates the waters of the coastal zone and its cleaning from the natural and anthropogenic pollution.

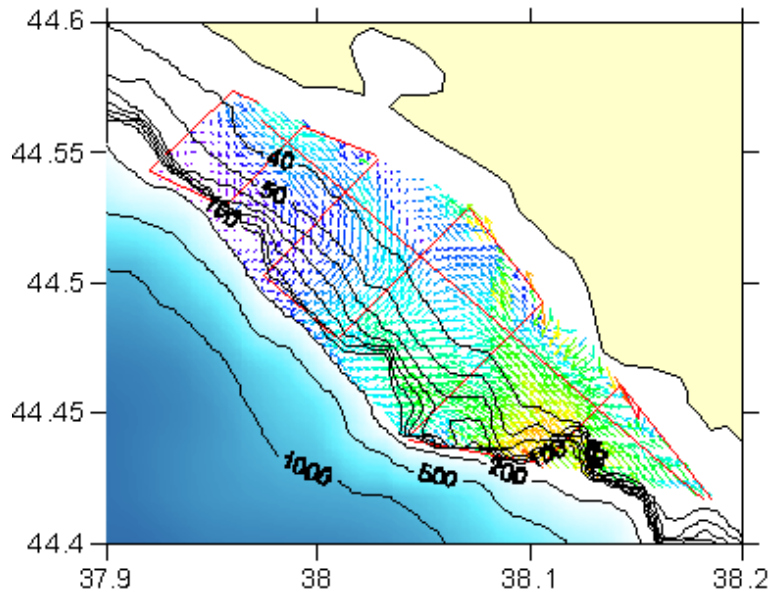


**Figure.** Horizontal currents on the shelf of the Black Sea based on the data of towed ADCP. The currents were averaged over the thickness of the upper layer ( $H = 20$  m). Red lines denote the lines of ADCP tows. Black lines are isobaths indicated with the depths in meters.

The calculations of surface currents were performed for the period 1998-2009. They were compared with the data of observations. It was found that the kinetic energy of the surface current is maximal in the winter period. It is twice more intense than in summer. In 2002-2003 a change in the circulation regime was recorded. In 1998-2002, the seasonal cycle of circulation was not clearly pronounced and the mean level of the kinetic energy was lower than in 2003-2009. These variations are related to the regime of large-scale wind forcing.

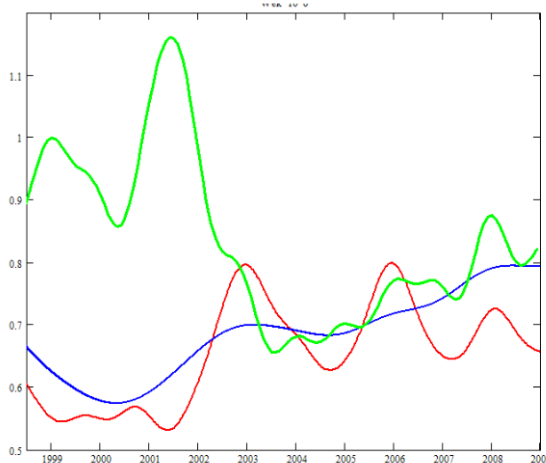


**Figure.** Chlorophyll concentration in relative units (green), kinetic energy of surface currents ( $E_k$   $10^2$  m/s) (red), and rate of Ekman energy pumping ( $W_E$   $10^6$  m/s) (blue).

## Wave interactions

A theory was developed that describes nonlinear interactions between free oceanic waves with wave modes, trapped in narrow waveguides, which exist in the ocean near elongated inhomogeneities (for example, near coasts, over steep topography, near the equator, etc.). Such interactions provide free energy exchange between the open ocean and waveguides. Despite their practical importance they remained poorly studied until present.

Theoretical studies of freak wave generation were performed. It was shown in the numerical experiment that the probability of extreme wave generation is related to the characteristics of spectrum and can be reliably estimated in the terms of two main dimensionless parameters: wave steepness and width of the spectral distribution. The theoretical investigations of the wind wave development allowed us to construct a self-consistent scheme based on the theory of weak turbulence, dimension theory, and results of numerical modeling. It was shown that wave growth can be presented as a sequence of reference regimes when integral wave momentum, energy, wind wave action play the determining role.

## Internal waves under ice

Dominating periods of short internal waves in an Arctic fjord under ice were studied in Spitsbergen. The period of these waves is estimated at a few minutes. These waves are generated due to instability of a large-scale flow. Short-period waves correspond to the waves with a dimensionless wavenumber equal to 0.5. The spectral level of vertical fluctuations caused by internal waves is determined by the wind and tide forcings. In winter, when the water level in the fjord is covered with snow the wind stress is not transferred to internal oscillations, and the spectral level of internal waves decreases.

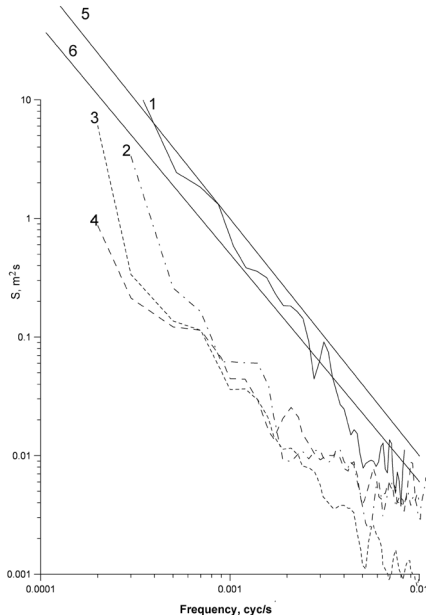
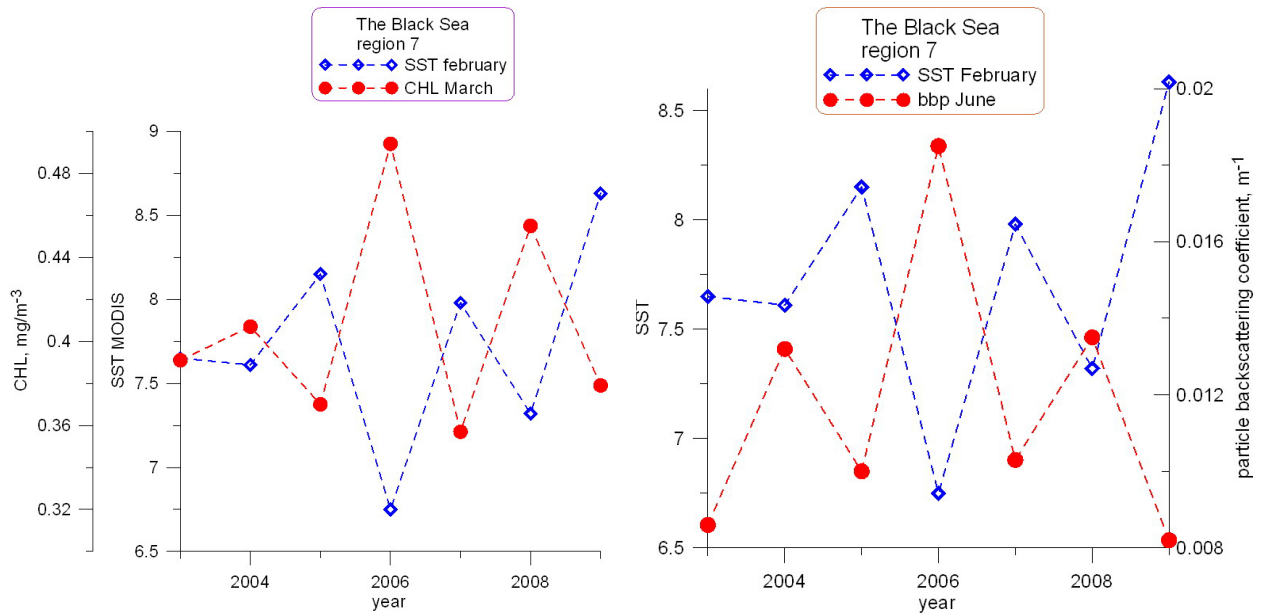


Figure. High-frequency spectra of vertical displacements based on the moored measurements in the fjord. (1) August 2009, two temperature sensors; (2) March 2008, one temperature sensor under ice; (3) March 2010, salinity sensor under ice; (4) March 2010, temperature sensor under ice; (5) Garrett-Munk spectrum in winter conditions; (6) Garrett-Munk spectrum in summer conditions.

## Satellite oceanography

A correlation was found between the winter sea surface temperature and intensity of spring plankton blooming as well as with the turbid surface water in June in the Black Sea. It is assumed that the initial cause of this correlation is intensification of winter convection during cold winters, which facilitates the supply of the upper sea layer with nutrients.



**Figure.** Comparison of interannual variations in the mean values of surface temperature in February (blue curves), chlorophyll concentration in March (left) and particle backscattering coefficient in June (right) in the eastern part of the deep-water Black Sea.

## Radar observations of the surface

Analysis of the radar data revealed that 90% of the eddy structures detected in the radar images of the Black and Baltic seas are visualized on the basis of the slick mechanism, and the remaining 10% on the basis of the shear wave mechanism.

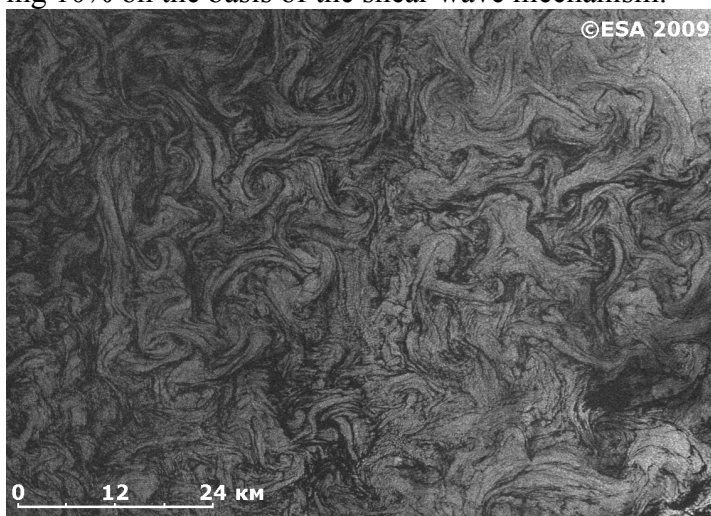


**Figure.** Submesoscale vorticity of surface currents in the Baltic Sea (dense package of mesoscale eddies (Envisat ASAR WSM, April 25,200; 09:09 GMT.). Spatial resolution is 75 m.

## Mathematical modeling

An information computational system of variation data assimilation was developed. It was shown that a notable change in the calculated characteristics occurs as a result of data assimilation. The model values approach the observations and the solution adequately reflects the observed structure of natural fields.

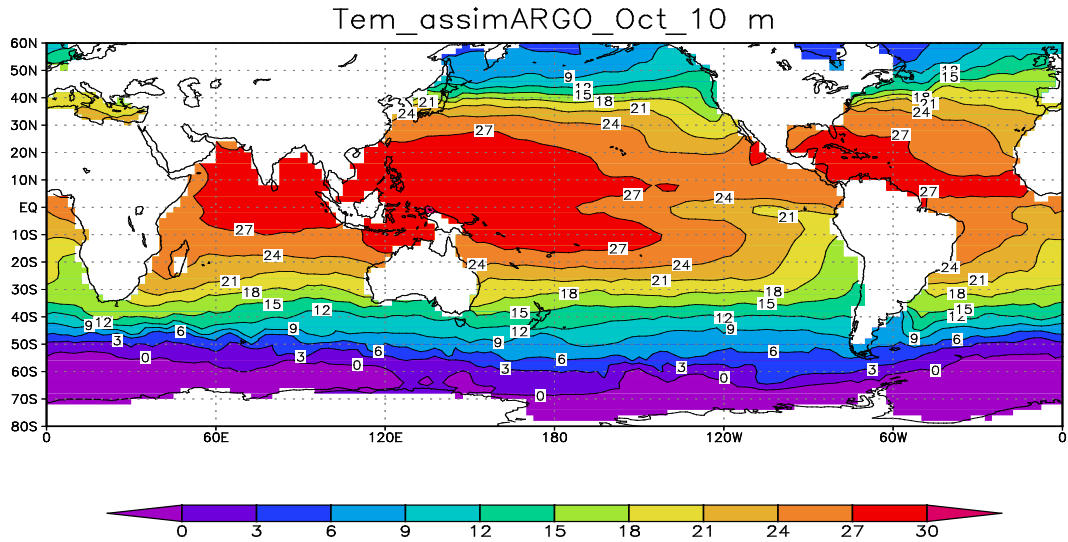


**Figure.** Temperature in the ocean at a level of 10 m (October). Solution of the variation assimilation of ARGO floats.

## Caspian Sea

Correlation between the hydrological regime in the Caspian Sea and large-scale atmospheric circulation were studied. The model experiments demonstrate a significant influence of the long-term Atlantic oscillation on the temperature regime over the basin of the Caspian Sea. A sigma-z version of the model was developed with the description of the flooding and drainage processes. Test calculations on restoring the inter-annual variability of the circulation and water level of the Caspian Sea demonstrate the reality of the numerical solution.

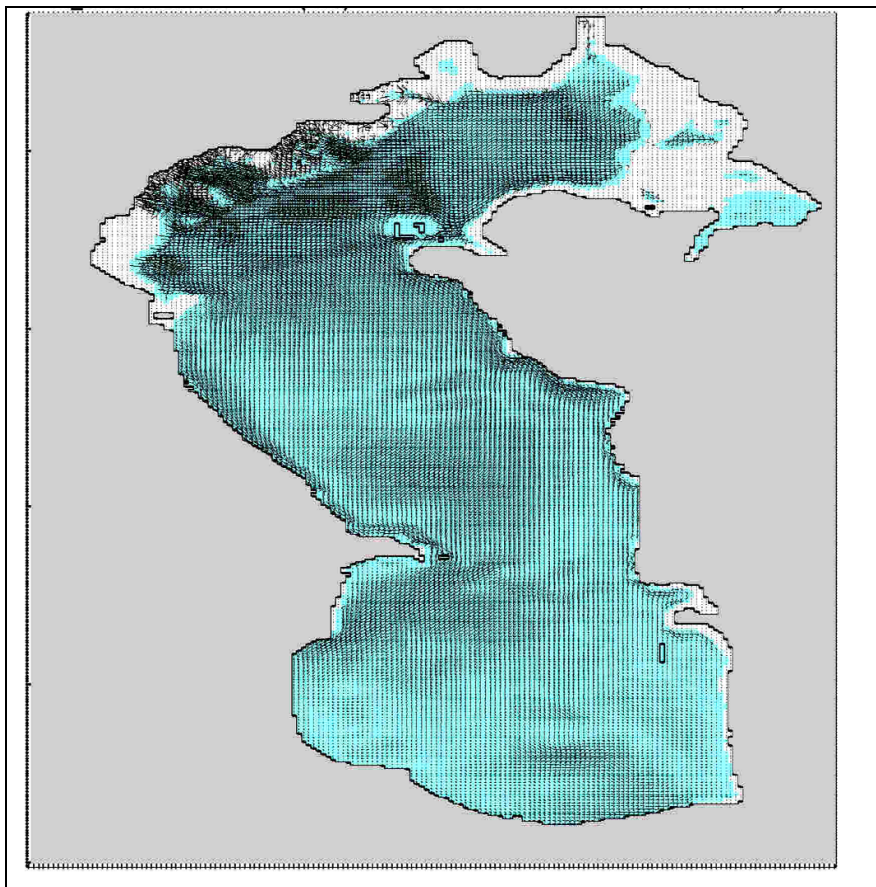


**Figure.** Surface currents of the Caspian Sea. The drained territory from 1964 compared with 1958 is shown.

A multidisciplinary expedition in the Caspian Sea was organized. The program of this expedition included investigations of the physical, chemical, sedimentological, and geological characteristics of the water, land, and bottom sediments. A system of sharp fronts was detected over the section across the mouth of the Volga River. It was shown that stationary currents between the thermocline and bottom exist within the main cyclonic gyre of the Middle Caspian Sea. These currents correspond to the direction of the cyclonic gyre. The currents are most intense in the layer 100-300 m. They are intensified in the cold seasons of the year and become weaker in warm seasons. Long-term observations demonstrate that the center of the cyclonic gyre is much closer to the western coast than it was considered before.

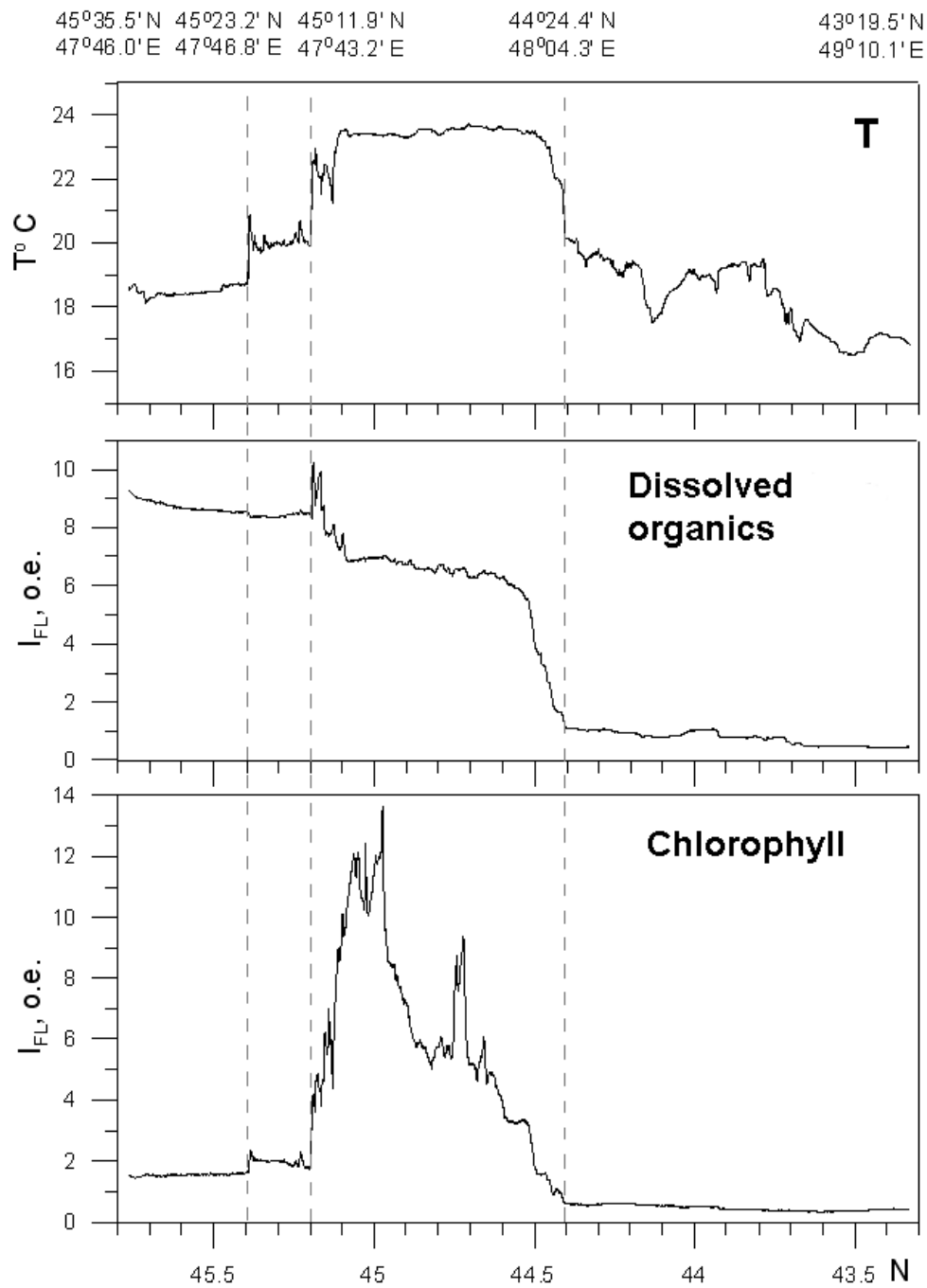


**Figure.** Distribution of chlorophyll fluorescence intensity (lower curve), dissolved organic intensity (middle curve) and temperature (upper curve) along the section crossing the frontal zone in the mouth of the Volga River. The measurements were made on June 4-5, 2010.

## Global circulation model

A new dynamic core for a 3D model of the World Ocean was developed. The model is developed for the system description of climate forming processes in the range from large-scale to mesoscale. Test experiments were carried out with a resolution of 1/8 deg. by 1/8 deg. by 32 levels.

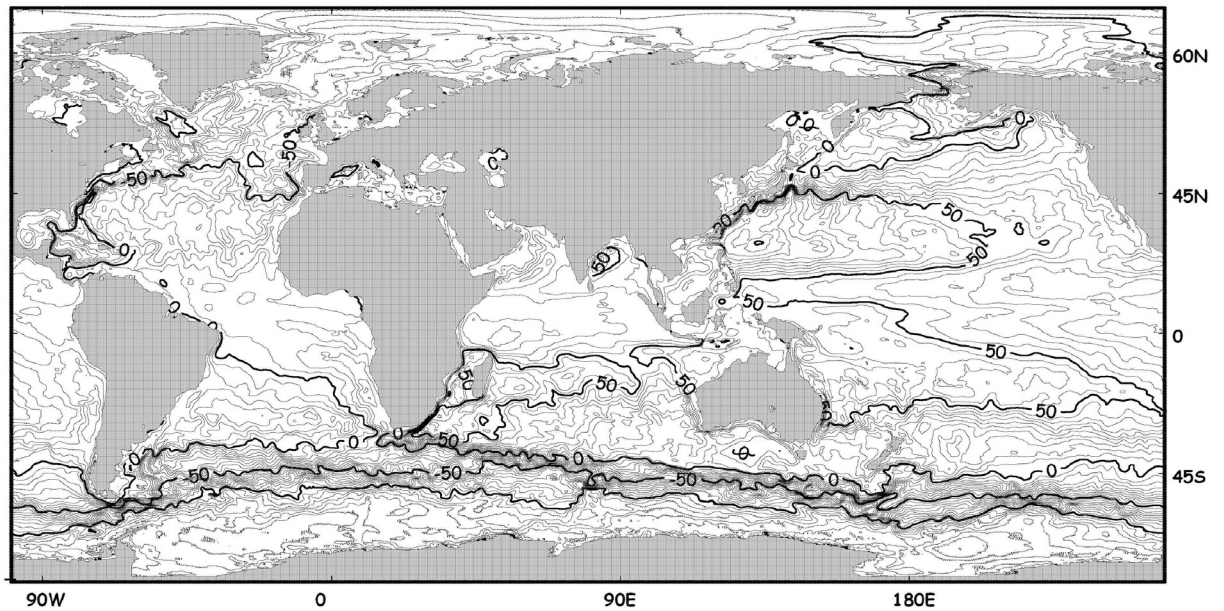
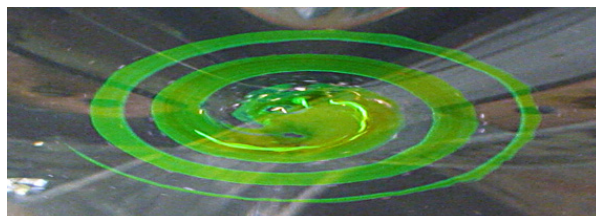


Figure. Sea level topography after 4 months of the model time. Solution of the World Ocean model 1/8 deg by 1/8 deg by 32 levels.

## Laboratory modeling

Modeling of the oil spill form at the ocean surface was performed, The transformation of oil spot entrained in the eddy motion was traced. The experiments allowed us to reproduce the oil transformation into elongated spirals. The transformation patterns in the natural and laboratory conditions are similar.



**Figure.** Spiral structures in Vityaz Bay (Pacific Ocean). Photo (left). Spiral structure of the uranyl solution from a compact patch in the center of eddy rotating anticlockwise (laboratory experiment) (right).

## Laboratory experiments

Laboratory experiments in a setup tank filled with salt water on a rotating platform confirmed the supposition that formation of the surface fresh layer found in the summer of 2007 in the southwestern part of the Kara Sea is related to the summer flooding of the Ob and Yenisei rivers. This is a powerful discharge of fresh water with different chemical composition and their further mixing.

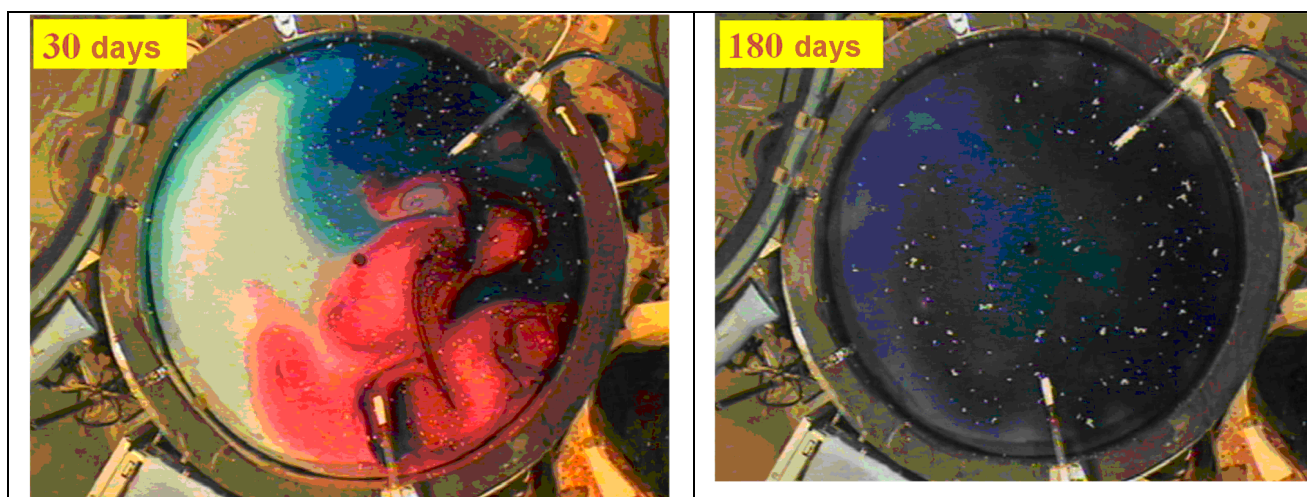


**Figure.** Interaction and mixing between two freshwater plumes in a laboratory tank (view from above) on a rotating platform initially filled with the salt water. The freshwater sourced (horizontal pipes) operate during 30 laboratory days (periods of the platform rotations) and then the freshwater supply terminates (30 days, left). The plumes (red and blue) have been formed already. Their eddy structure is complicated. Due to the eddy interactions mixing occurs between the plumes, which terminate after 180 laboratory days.